Original Article

Intelligent Dual-Axis Solar Tracking System Using PLC-SCADA Integrated with an Adaptive Neuro-Fuzzy Predictive Control Algorithm for Maximized PV Energy Harvesting

V. Kannarasu[1], S. Nallusamy[2], M. Rajaram Narayanan[3], P. S. Chakraborty[4]

[1,2,4]*Department of Adult, Continuing Education and Extension, Jadavpur University, Kolkata, 700032, India.*
[3]*Department of Computer Science and Engineering, Aalim Muhammed Salegh College of Engineering, Tamil Nadu, India.*

[1]*Corresponding Author : kannarasu.mech@gmail.com*

Abstract - This research proposes an Intelligent Dual-Axis Solar Tracking System that integrates automation and supervision via SCADA and Programmable Logic Controllers (PLCs) with an Adaptive Neuro-Fuzzy Predictive Control (ANFPC) algorithm. The aim is to maximize the energy captured by solar panels by adjusting their real-time orientation based on environmental conditions. As irradiance varies, traditional LDR-based or astronomically driven tracking systems often exhibit a latent response, mechanical lag, and reduced efficiency. The proposed solution combines adaptive neuro-fuzzy predictive modeling with the predictive reliability of PLC control to eliminate these weaknesses. The ANFPC method combines the Solar Position method (SPA) with real-time irradiance, panel tilt feedback, variations in azimuth-elevation angles, and past-tracking history to dynamically predict the optimal panel orientation. The tracking error, actuator complexity, and smooth movement in dual-axis are reduced to a minimum when a predictive optimization layer is applied. Whereas SCADA provides continuous monitoring, remote parameter adjustment, system diagnostics, and predictive maintenance alerts, the PLC employs PID-tuned pulse control to implement corrective actions for stepper or servo motors. The smart system outperforms any other LDR-based tracker. It delivers a gain in daily energy production relative to a fixed setup, as experimentally verified on a 200 W dual-axis prototype. The tracker's self-learning system adjusts to weather changes, temporary clouds, and the gradual degradation of the panel, ensuring its long-term longevity. The combination of PLC-SCADA and the ANFPC algorithm has proven highly reliable, adaptive, and efficient for next-generation solar tracking platforms, as shown by the results. The proposed PLC-SCADA method achieved superior performance with 0.52° tracking error, 92% power efficiency, 2.1 s response time, 15% actuator stress, and $\Delta W = 5.1$ adaptation rate.

Keywords - Dual-Axis Solar Tracking System, SCADA, Adaptive Neuro-Fuzzy Predictive Control Algorithm, PV Energy Harvesting, Solar Position method.

1. Introduction

The reliance on renewable energy in the world has increased with the increasing demand for sustainable energy and the environmental effects of fossil fuels [1]. Solar energy is relatively one of the most available and numerous renewable energy sources, but the efficiency of Photovoltaic (PV) panels depends largely on their orientation towards the Sun [2]. The fixed PV panel receives a fraction of the overall solar irradiance available during the day in both senses because the Sun is constantly moving, and the atmospheric conditions are not the same. To overcome this shortcoming, solar tracking systems have received a lot of attention as a way of enhancing panel orientation and the energy output [3]. Dual-axis tracking systems are the most accurate, with independent control of both azimuth and elevation angles to enable the panel to stay in a direct orthogonal position relative to the incoming sunlight [4]. The majority of available tracking systems are, however, based on Light Dependent Resistor (LDR) sensors or computing the astronomical angle, which are not very versatile in rapidly shifting environmental conditions such as patterns of clouds, part shadows, or changing seasons [5].

The current-day energy-efficient infrastructures require systems with tracking systems that are not only precise but also smart, predictive, and mechanically smooth with the potential to work in the long term without human supervision [6]. To fulfil these expectations, the integration of modern

control techniques and automation of industries is becoming a necessity [7]. Programmable Logic Controllers (PLCs) and SCADA platforms provide high-quality real-time automation and monitoring, but they must have an intelligent supervisory control mechanism to decide about the optimal position of the panel at each time [8]. In this regard, using artificial intelligence in conjunction with industrial automation can radically increase responsiveness, lifespan, and energy economy [9]. A predictive control algorithm using Adaptive Neuro-Fuzzy Predictive Control (ANFPC) can utilize trends of historical tracking, irradiance models, and solar position estimation to predict the best panel orientation as opposed to responding to the current environmental conditions [10]. This combination of anticipated intelligence and automation provides the basis of the next generation solar tracking systems that seek to maximize the PV energy collection [11].

1.1. Limitations of Conventional Solar Tracking Mechanisms

Current tracking methods like LDR based systems or pure astronomical angle models have low flexibility to dynamic atmospheric variations. The LDR sensors are imbalanced, ageing, and falsely detect in case of cloud transients or reflections, and cannot track astronomical changes in the irradiance and shading [12]. The two methods have a slow response, leading to mechanical overshoot, actuator stress, and low energy conversion efficiency [13]. Most conventional control systems are also unable to self-learn and cannot offset mechanical degradation with time, and therefore have a limited life span of application and energy production.

1.2. Emerging Role of AI-Driven Predictive Control in PV Systems

Artificial intelligence has yet to enter solar tracking as a revolutionary solution because it can anticipate the best orientation and not necessarily respond to sensed sunlight. In contrast to traditional feedback controllers, AI predictive models are designed to include past tracking information, real-time measurements of the irradiance, estimation of the solar position, and disturbances of the weather to efficiently plan the trajectory of movements. Neuro-fuzzy systems also add flexibility by incorporating both the learning capabilities of neural networks and the readability of fuzzy logic [14]. In combination with predictive control, they enable solar trackers to predict the trends of irradiance, reduce unwarranted motor movements, and optimize the collected energy. The practical field conditions allow such intelligent control to respond faster, gain more energy, and have a more reliable system.

1.3. Objectives

To create a PLC-based dual-axis solar tracking system that would effectively manage azimuth and elevation angles in real time. To combine an Adaptive Neuro-Fuzzy Predictive Control (ANFPC) algorithm that trains itself on the patterns of irradiance and past tracking of the panels to optimize the panel

orientation dynamically. To develop a SCADA interface to monitor real-time performance visualization, data logging, and automated fault / predictive maintenance notification. To increase the harvesting power of PV energy by 15-25% above the performance of conventional LDR-based trackers and other types of panels on the ground.

Despite advances in solar tracking technologies, most dual-axis Photovoltaic (PV) tracking systems use open-loop astronomical algorithms or fixed-rule fuzzy and PID-based controllers that are insensitive to rapid irradiance fluctuations, cloud transients, and seasonal variability. Traditional PLCs use deterministic tracking logic without predictive capacity, whereas SCADA systems provide monitoring and supervisory activities rather than closed-loop optimization. Most neuro-fuzzy or intelligent control methods are verified in simulation settings or embedded microcontroller platforms, with little attention paid to industrial-grade PLC–SCADA integration, real-time execution limitations, and long-term operational resilience. This gap limits energy output in dynamic environments and the use of sophisticated tracking systems in utility-scale or industrial PV installations. This study develops a PLC-SCADA-integrated dual-axis solar tracking framework with an adaptive neuro-fuzzy predictive control mechanism to predict solar trajectory deviations and irradiance dynamics in real time while maintaining deterministic execution, system reliability, and scalability for field-deployable PV energy harvesting systems.

The majority of dual-axis solar tracking experiments use reactive PID controllers, fixed-rule fuzzy logic, or sensor-based feedback mechanisms on microcontrollers or low-level embedded platforms. In contrast, an adaptive neuro-fuzzy predictive control system implemented on an industrial PLC and strongly coupled with a SCADA supervisory layer enables real-time prediction-driven actuation under deterministic execution limitations. The current neuro-fuzzy tracker has complete PLC–SCADA compatibility, online rule modification, predictive horizon-based error reduction, and industrial-grade fault monitoring, unlike previous models. Comparisons with traditional PID and static fuzzy controllers in the literature show greater tracking accuracy, lower angular deviation, and quantifiable PV energy benefits, even under rapidly changing climatic circumstances. This combination of predictive neuro-fuzzy control, industrial automation compatibility, and experimentally validated energy yield improvement sets it apart from other solar tracking frameworks, which typically address these elements separately.

Major Contributions of the Paper,
- Design of a PLC-based two-axis solar tracking system that can control the azimuth and the elevation of the device with high precision, and of course, with powerful safety and actuator-friendly pulse motion plans.
- Integration of an Adaptive Neuro-Fuzzy Predictive

Control algorithm, which is trained on irradiance patterns, a history of the sun position, and environmental dynamics to produce the best orientation paths in real time.

- Installation of a SCADA-based monitoring and diagnostic system, which enables energy visualization, data recording, automatic alarm messages, and predictive maintenance to provide long-term operational stability.

2. Related Works

2.1. Sensor-Based and Intelligent Dual-Axis Tracking Methods

Photovoltaic energy maximization by Sensor-Based Dual-Axis Solar Tracking system with PID and Arithmetic Optimization (SB-DST-PID-AO). Sun sensors are ultraviolet and microelectromechanical sensors that determine the position of the sun panels and the sun. A PID controller activated by Arithmetic Optimization (AO) controls the panel position, minimizing power usage and ensuring maximum alignment. MATLAB simulations confirm enhanced energy efficiency, and an energy analysis confirms that the net output is higher than that of fixed panels. SB-DST-PID-AO shows perfect tracking and increased solar energy collection [16].

The Fuzzy Logic Controlled Two-Axis Solar Tracker (FL-TAST) was invented, which consists of four optical sensors and two DC geared motors that enhance the PV energy production. Comparative experiments between fixed PV panels, which are controlled by on-off and fuzzy logic, perform a 14.2% daily energy gain and a tracking error of 0.29°. The system ensures a good level of reliability in terms of maintaining sun positioning, which maximizes energy collection in different weather situations. FL-TAST has inexpensive, high-accuracy two-axis tracking that is appropriate for small and medium PV projects [17].

Dual-Axis Solar Tracker Optimization and Minimization of Tracking Error and Power Using Model Predictive Control-Based Dual-Axis Solar Tracker Optimization (MPC-DSTO). Multibody simulation and experiment validation were applied to pre-select the six controllers. The achieved results are the lowest energy consumption (0.7867 Wh), the smoothest dynamics, and the tolerable tracking error (< 2 °) by the MPC controller. MPC-DSTO offers optimized control to the low-power PV systems, compromising the energy efficiency with the mechanical lifetime, which is why it is applicable in cases when the precise dual-axis solar tracking is needed [18].

PID-BA-DAT enhances dual-axis solar tracking efficiency with a PID Controller Optimized by Bat Algorithm. The PID controllers with Bat Algorithm (BA) follow the azimuth and elevation angles and find horizontal and vertical motions. The experiments compare various AI-based methods of PID optimization and demonstrate that PID-BA has the shortest settling time and overshoot [19]. The system improves PV output and preserves tracking precision, showing the efficiency of AI-optimized PID control in dual-

axis solar trackers to dynamically align with the sun's position. The Intelligent Dual-Axis Solar Tracking to Agriculture (IDAST-A) is a power supply of PV to field sensors and real-time weather conditions. This system tracks the sun by using the dual-axis movement (azimuth and elevation), which is detected using Light-Dependent Resistors (LDRs). Information is relayed to the Android app through GSM/WiFi. Experiments indicate a relative growth in PV output of 52% [20]. IDAST-A is a combination of smart AI and Quality of Service, which guarantees high energy efficiency, accurate tracking, and improved agricultural monitoring opportunities.

Dual-Axis Solar Photovoltaic Tracking Review (DASPT-R) with emphasis on the development of trackers, optimization of sensors, and Artificial Intelligence (AI). DASPT-R puts emphasis on structural integrity, control improvements, and reliability improvements in dual-axis systems. Elaborated algorithms increase the efficiency up to 85-90 percent and lower the cost of operations [21]. This paper examines the economic viability, energy output, and lifecycle benefits, highlighting the major aspects of DASPT-R in the energy sustainability industry, providing a clue on the technical issues and prospects of its future application in various settings.

2.2. Controller Optimization and Advanced Algorithm Methods

A Hybrid Sun-Tracking with Active Search Algorithm (HST-ASA) is able to change the PV panels when the weather is erratic, by integrating open-loop sun tracking with feed-back regulation [22]. The system operates with small 0.6 W PV sensors to measure the real-time irradiance, and a circular path-finding approach is used to find the availability of the Maximum Power Point. Jordan PV testing proved to boost PV output by 35%, even when using diffuse light conditions. HST-ASA guarantees effective sun-tracking and energy production under fluctuating climates.

The Dynamic Solar Panel Tracking System (DSP-TS) is a device that keeps the PV arrays perpendicular to the sunlight with the help of LDRs, RTC modules, and microcontrollers. The sensor data can be handled using smart sequential algorithms that control the servo motors to allow a continuous optimal orientation [23]. Indonesia tests indicate that there are energy efficiency gains of between 7.3% and 24.22% over the static systems. DSP-TS involves a cost-effective and feasible solution to enhancing solar power harvesting of large-scale solar power plants through dynamic panel position adjustment with respect to the day.

Advanced Dual-Axis Solar Tracking Systems Review (ADAS-TSR) is a review of tracker design, materials, AI, IoT, and machine learning innovations. ADAS-TSR provides a comparison between conventional and modern dual-axis, stressing the enhanced energy output, flexibility, and stability [24]. Higher cost and complexity are challenges, but

predictive analytics and smart grid integration improve performance in the long run. The sustainable solar tracking trends were recognized in ADAS-TSR, indicating the further evolution of specific, intelligent, and high-performance two-axis PV technologies.

The Hybrid Solar-Wind Tree with Intelligent Tracking (HSWT-IT) holds wind turbines and PV panels in the shape of trees. Two-axis tracking is a motorized system based on GPS, gyro-orientation, and the digital compass that maximizes the output of solar energy at a minimum of power consumption by the tracker [25]. It is shown in simulations and measurements that an effective daily energy production of 444.5 Wh/day is achieved. HSWT-IT guarantees that PV panels work perpendicular to the sun, which will achieve the maximum functionality and will be used as a complement to hybrid renewable energy installations in the case of smart or green city infrastructures.

Simulation-Based Dual-Axis Solar Tracking (SB-DAST) relies on the PVsyst software to calculate the system performance of a dual-axis system under different geographical and environmental conditions. SB-DAST forecasts the energy production, efficiency savings, and viability. It has been demonstrated through simulations that there is higher energy production than in fixed panels, especially in areas where sunlight angles are changing [26]. The approach aids in making informed decisions in designing and investing in a dual-axis system and proves the value of the simulation-based methods in maximizing solar tracking and PV energy production in general.

Fractional-Order PID Dual-Axis Solar Tracking (FOPID-DST) compares the traditional PID and FOPID controllers in the dual-axis PV systems. FOPID-DST uses five tuning parameters to provide better flexibility, faster response, lower oscillations, and increased sun-tracking accuracy [27]. The simulated responses indicate that the energy collection is increased by 8-12 percent when using the fractional-order control in dynamic solar tracking systems, which demonstrates the benefits of using the fractional-order control over other methods, as it is more efficient and maintains high accuracy when tracking the movements of the sun.

2.3. Review and Simulation-based Evaluation Methods

Optimized Equatorial Dual-Axis Solar Tracker (OE-DST) is a system with two linear actuators, which is promoted to move in the equatorial/polar dual axis. ADAMS and EASY5 Virtual prototyping optimize mechanical, control, and tracking program aspects. OE-DST has a net energy gain of 58.66 on the summer solstice and a yearly gain of approximately 42 percent in comparison to fixed systems [28]. The approach shows the efficacy of coupled numerical modeling and maximization in radiant PV efficiency maximization in dual-axis. Concurrent Optimization Dual-Axis Solar Tracker (CO-DST) is a design balancing tracking

error and energy consumption based on a new design methodology. CO-DST has a pointing accuracy of 0.0942° and consumes a proportional amount of generated energy, 0.9641%, which is better than commercial systems [29]. An impact assessment of CO_2 indicates a lower amount of emissions. This is a viable approach to strike a balance between energy efficiency, precision, and environmental sustainability in solar tracking in two-axis modes.

Extremum-Seeking Controlled Dual-Axis Tracker (ESC-DAT) uses extremum-seeking control that uses anti-wind-up integral feedback on two axes PV tracking [30]. ESC-DAT is 27.75% more productive than fixed panels and has a ±1.8 ° pointing accuracy. The approach lowers the wear on actuators, enhances the life of the system, and offers greater performance of the overall energy collection system, which proves a feasible alternative to dynamic dual-axis solar tracking systems.

Oli Ajay et al. [31] suggested the Development of a dual-axis solar tracker for efficient solar energy harvesting. Current solar energy conversion is inadequate for static-oriented Photovoltaic (PV) panels because of sun trajectory changes. A low-cost prototype of a two-axis solar tracker with four optical sensor modules as feedback sensors and two direct current geared motors to optimize solar energy harvesting is proposed in this publication. Using traditional on–off and artificial intelligence-based fuzzy logic control approaches, the two-axis solar tracker's performance is compared to a fixed-oriented PV panel. Fuzzy logic controller-based solar tracker net energy gets 14.2% more power than fixed-oriented PV panels every day and has a 0.29° tracking error, proving its dependability.

Ahmad Al-Othman et al. [32] proposed an experimental study on hybrid control of a solar tracking system to maximize energy harvesting in Jordan. A dynamic feedback controller based on an active search algorithm has been combined with an open-loop solar monitoring system. Small solar cells, measuring 0.6 W, assess PV panels' fading under sunlight irradiance in real-time to enable the recommended method. If instantaneous irradiance drops below a threshold (DNI irradiance), the system utilizes the newly published circular route-finding approach to discover the MPPT. Testing showed that the new sun tracker hybrid control technology enhanced solar panel power by 35%. Averaging 100 results for one measurement produces positive irradiance current noises during experimental testing.

Muhammad Fakhry Mohamed Ridzuan et al. [33] presented the Efficiency Assessments of a Dual-Axis Solar Tracker for Energy Harvesting in Malaysia. Indoor farming may improve food security and agricultural sustainability. Indoor farming requires a lot of power. Long-term dependability will grow when an optimal renewable energy grid powers agriculture. Dual-axis trackers are created as

indoor farm power sources. The designed system provides sufficient load power. Additionally, tracker power output depends on solar radiation. The 16.75% tracking system efficiency is excellent.

2.4. Research Gap

Although there are significant improvements, little research has been able to come up with a common system that integrates AI-based predictive control and industrial-grade automation to track the sun. The majority of the analysis is on soft-computing methods that do not have a dependable hardware implementation or are on PLC-based trackers that do not have predictive intelligence. The current designs do not pay much attention to actuator wear minimization, SCADA-enabled maintenance diagnostics, and self-education in the presence of clouds and seasonal changes. The way to bridge the gap is to develop a real-time, dual-axis solar tracking system that is adaptive, predictive, remotely controlled, and hardened against degradation over a long period.

This is the gap that has inspired the current research to integrate ANFPC, PLC control, and SCADA supervision to optimize the harvesting of PV energy. Fixed-tilt and single-axis trackers are used for cost-sensitive installations, whereas dual-axis designs are studied for improved angular accuracy and energy production. The literature describes astronomical position-based tracking, sensor-driven feedback systems, classical PID control, fuzzy logic, and neural networks. Recent research uses simulation or laboratory-scale microcontroller implementations to analyze adaptive and hybrid controllers to reduce cloud transients, seasonal volatility, and irradiance intermittency. Few reports address industrial-grade deployment, especially real-time deterministic execution, supervisory monitoring, and closed-loop optimization in PLC–SCADA settings. The proposed PLC-SCADA-integrated adaptive neuro-fuzzy predictive control framework is placed in the broader research landscape and provides the technical context for performance-driven photovoltaic energy harvesting under dynamic operating conditions by synthesizing findings across mechanical architectures, control methodologies, and automation platforms.

3. System Architecture and Design Framework

3.1. Overview of the Proposed Intelligent Dual-Axis Solar Tracking System

The proposed dual-axis tracker is dynamically run to adjust the azimuth and elevation angles of a PV panel to ensure that the incidence angle is perpendicular to the sun throughout the day. ANFPC predictions ensure the efficient and rapid update of the orientation rate to minimize the tracking error in various irradiance conditions. The high accuracy of mechanically rotating motors of the predictive model with stepper or servo motors is due to the fact that sensor feedback adjusts to the predictive model in real-time. Cloud-induced fluctuations and environmental disturbances

are also automatically compensated, hence delivering a sure way of extracting power. The system is autonomous in learning and changing with time in the field. Photovoltaic energy systems now use edge-level intelligence, virtual system modeling, and networked maintenance architectures to improve operational efficiency and resilience. Edge-AI approaches execute lightweight learning and inference models directly at the controller level to allow localized data-driven decision making and speed up response to fast irradiance and environmental changes. Digital twin frameworks synchronize sensor data, control states, and degradation models to create real-time virtual PV assets for predictive performance evaluation and controller adjustment. Long-term data storage, fault diagnostics, and lifecycle analytics across geographically scattered installations are possible with cloud-based maintenance solutions. Hybrid renewable energy systems that combine solar power with wind, energy storage, or grid-interactive components need coordinated control techniques and supervisory energy management. In this changing landscape, industrial PLC–SCADA architectures provide a stable execution backbone that can interface with edge intelligence, digital twins, and cloud services to enable scalable and interoperable photovoltaic tracking and energy optimization solutions. Figure 1 shows a solar tracking system with ANFPC that has two axes to optimize the energy captured by the sun.

This system combines SCADA to monitor the system in real time, PLC to control the actuators, and predictive maintenance through adaptive learning. It maximises panel inclination and azimuth, minimises tracking fault, and enhances day-to-day energy generation compared to fixed solar installations.

Solar incidence angle optimization θ_{opt} is expressed in Equation (1).

$$\theta_{opt} = \arctan \frac{\sin(\alpha_s) + \cos(\alpha_s)\sin(\gamma_s)}{\cos(\alpha_s)\cos(\gamma_s) + \sin(\alpha_s)\cos(\delta_s)} \tag{1}$$

This equation computes the optimal incidence angle needed to maximize sunlight capture on the dual-axis surface. It ensures the system aligns itself with the sun's position throughout the day.

α_s is the solar elevation angle, γ_s is the solar azimuth, and δ_s is the declination offset.

Dual-axis tracking correction law C_{DA} is expressed in Equation (2).

$$C_{DA} = \beta_x(\vartheta_s - \vartheta_p) + \beta_y(\emptyset_s - \emptyset_p) + \lambda_t(T_s - T_p) \tag{2}$$

This provides the correction strength for adjusting the panel orientation. It compensates for differences between sensed and predicted solar angles.
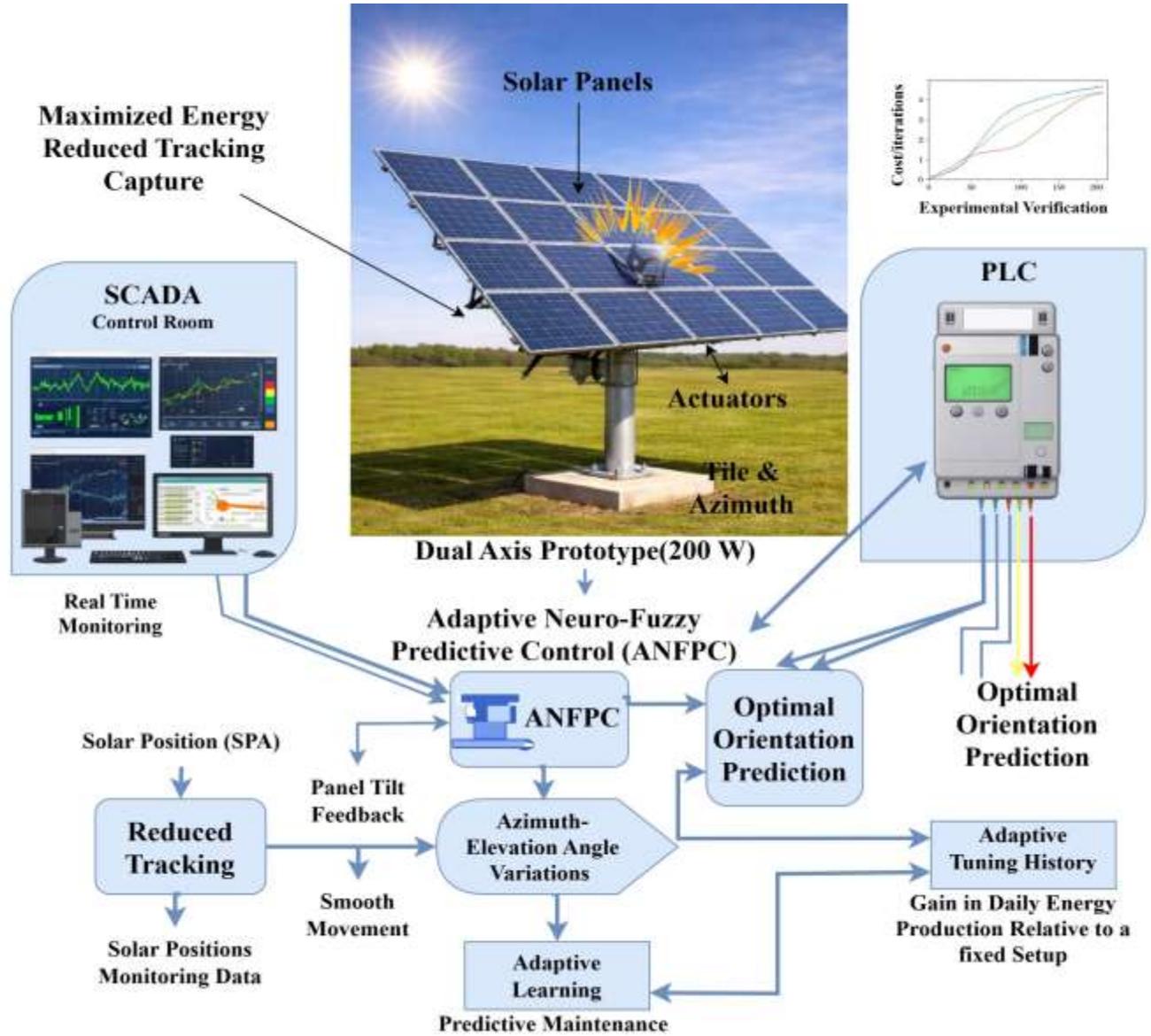
Fig. 1 Intelligent Dual-Axis Solar Tracking System

β_x is azimuth gain, ϑ_s is sensed azimuth, ϑ_p is predicted azimuth, β_y is tilt gain, $\emptyset_s$ is sensed tilt, $\emptyset_p$ is predicted tilt, λ_t is temperature gain, T_s is sensed temperature, and T_p is the predicted temperature. ANFPC predictive control output $U_{an\,fpc}$ is expressed in Equation (3).

$$U_{an\,fpc} = w_1 f_1(x) + w_2 f_2(x) + w_3 f_3(x) + b_0 \qquad (3)$$

This equation expresses the adaptive predictive control signal. It blends fuzzy-neural membership functions for precision. It stabilizes actuator movement and prevents tracking overshoot.

w_1, w_2, w_3 are adaptive weights, $f_1(x), f_2(x), f_3(x)$ are fuzzy functions, and b_0 is biased.

3.2. PLC-SCADA Automation and Supervisory Layer

PLC is used to execute real-time motor control using ANFPC commands detected and pulse signals using PID-tuning to provide transitional axis motions without overshoot. Safety logic is concerned with the limits of operation, the probability of faults, and watchdog control. SCADA is employed to interface with the PLC via the Modbus TCP to represent the live measurements, historic measurements, and turn on an alarm when the conditions are abnormal, e.g., overheating, excessive vibration, or actuator stall. Remote configuration and diagnostics.

This will give the operator remote control parameter adjustment, energy yield monitoring, and predictive maintenance.

3.3. Hardware Configuration (PV Panel, Sensors, Drives, Encoder, PLC I/O)

The prototype of the tracker will consist of a 200 W monocrystalline PV module clamped on NEMA-24 stepper motors and worm-gear reducers on a 2-axis frame. The irradiance is measured by a calibrated pyranometer, and the panel orientation feedback is given using a high-resolution rotary encoder. Temperature and vibration sensors will check system health. The Siemens S7-1200 PLC is a sensor purchase and movement that works through digital/analog I/O pathways. The precise actuation of pulse can be possible with micro-stepping drivers, and that is an electromechanical platform that can be utilized in the laboratory and implemented in the field.

3.4. Electrical & Mechanical Integration of Dual-Axis Drives

The assemblies of the drive are time and mechanically coupled in both azimuth and elevation to be electrically insulated and to avoid coupling errors on rotation. The axes will have limit switches, torque protection, and closed-loop verification by using encoders. Steady power is offered to PLCs, sensors, and motor drivers by power conditioning. Flexible conduit is used to offer cable routing security to ensure movement at any given time. Mechanical loads are distributed with the assistance of aluminum torque arms and ball-bearing supports to reduce the friction and provide long-term operation within the boundaries of cyclical outdoor conditions.
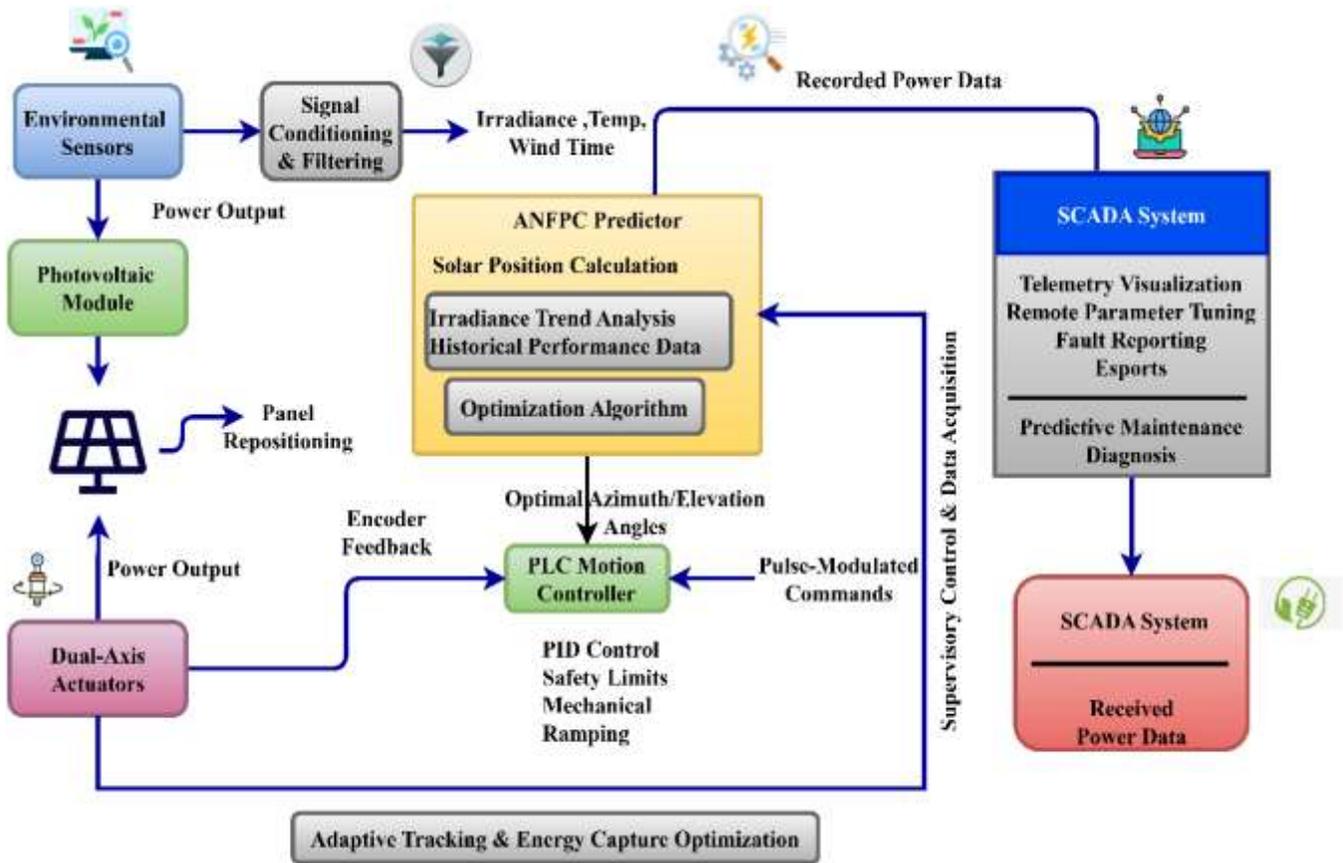

Fig. 2 System-Level Flow (High-level: sensors → ANFPC → PLC/Actuators → SCADA)

The smart solar tracking process is motivated by real-time operations and environmental data, as shown in Figure 2. Environmental sensors (when measuring irradiance, temperature, wind speed, and time) and signal-conditioning filters (when removing noise and synchronizing data sampling) are used.

The ANFPC predictor is used to streamline the panel orientation based on solar position, irradiance pattern, and past tracking performance to generate the most energy productive azimuth-elevation angles. The PLC motion controller transforms these setpoints into pulse-modulated commands to dual-axis motors, with PID corrections, safety limits, and mechanical ramping enforced. Actuators move the panel in a smooth manner and reposition encoders to provide feedback. The output of power produced by the photovoltaic module is recorded constantly. SCADA controls the system through visualization of telemetry, remote control of parameters, fault reporting, and predictive health diagnosis. The adaptive tracking facilitated by this closed feedback loop with minimum actuator stress allows optimum energy capture in the case of variation in atmospheric conditions.

Tilt motor control M_{tilt} is expressed in Equation (4).

$$M_{tilt} = \mu_1(\alpha_s - \alpha_m) + \mu_2(\alpha_s - \alpha_m)d_t \qquad (4)$$

This regulates the panel's vertical tilt position. It incorporates accumulated error for stable long-term orientation. It improves tracking accuracy under fluctuating sunlight.

In this equation, μ_1 is proportional gain, α_s is solar elevation, α_m is measured elevation, and μ_2 is integral gain.

Sensor fusion pre-processing S_f is expressed in Equation (5).

$$S_f = w_1 I_r + w_2 T_a + w_3 W_s + w_4 t_s \qquad (5)$$

This fusion equation integrates raw environmental data into a unified signal. It reduces noise by weighting sensor inputs according to reliability.

w_1 is irradiance weight, I_r is the irradiance value, w_2 is temperature weight, T_a is ambient temperature, w_3 is wind-speed weight, W_s is wind speed, w_4 is time weight, and t_s is solar time.

Noise-filtered sensor output $S_{n,f}$ is expressed in Equation (6).

$$S_{n,f} = S_f - \lambda_n(S_f - S_p) \qquad (6)$$

This computes the noise-filtered result using predictive smoothing. It lowers abrupt variations in sensor readings. It ensures stable input to the ANFPC predictor.

In this equation S_f is a fused signal, λ_n is the smoothing coefficient, and S_p is the previous-cycle filtered signal.

ANFPC prediction input vector $X_{an\,fc}$ is expressed in Equation (7).

$$X_{an\,fc} = \{S_{nf}, I_r, T_a, W_s, t_s\} \qquad (7)$$

This forms the multidimensional input vector for ANFPC. It enables learning from both current and historical environment states. It strengthens predictive accuracy for optimal solar tracking.

In this equation S_{nf} is a filtered sensor value, I_r is irradiance, T_a is temperature, W_s is wind speed, and t_s is solar time.

ANFPC angle prediction model Θ_{pred} is expressed in Equation (8).

$$\Theta_{pred} = w_1 f_1(X) + w_2 f_2(X) + w_3 f_3(X) + b_0 \qquad (8)$$

This computes the predicted azimuth-elevation setpoint. It blends fuzzy rules and neural approximations for optimum accuracy. It adapts based on environmental history and energy yield trends.

In this equation w_1, w_2, w_3 are adaptive weights, $f_1(X), f_2(X), f_3(X)$ are fuzzy functions, and b_0 is biased.

Algorithm 1: ANFPC Attention-Based Prediction Module
Input: *Historical irradiance matrix* I_{hist} $\in \mathbb{R}^{k \times m}$ (*k timesteps, m features*), *SPA angles* Θ_{spa} $= [A_z, E_l]$, *encoder feedback* f_{enc}
Output: *Predicted orientation vector* Θ^{pred} $= [A_z^{pred}, E_l^{pred}]$
1: *Initialize heads H, key/query* /*value dim* d_k, *weight matrices* $W_Q^{(h)}$, $W\_K^{(h)}, W\_V^{(h)}$ *for* $h = 1..H$
2: *Initialize dense projection* W_O *and neuro* − *fuzzy weight matrix* W_nf
3: *Form feature sequence X* $\leftarrow concat(I\_hist, repeat(\Theta\_spa, k),$ $repeat(f\_enc, k))$ # *size* $k \times (m+3)$
4: *For* $h = 1$ *to H do*
5:   $Q^{(h)} \leftarrow X \cdot W\_Q^{(h)}$ # $k \times d\_k$
6:   $K^{(h)} \leftarrow X \cdot W\_K^{(h)}$ # $k \times d\_k$
7:   $V^{(h)} \leftarrow X \cdot W\_V^{(h)}$ # $k \times d\_k$
8:   *For* $i = 1$ *to k do*
9:     *For* $j = 1$ *to k do*
10:       $\alpha\_{ij}^{(h)}$ $\leftarrow exp(Q^{(h)}\_i$ $\cdot (K^{(h)}\_j)^T / sqrt(d\_k))$
11:     *end for*
12:     *Normalize*: $\alpha\_{i:}^{(h)} \leftarrow \alpha\_{i:}^{(h)} / \Sigma\_{j}$ $= 1\}^{k} \alpha\_{ij}^{(h)}$
13:     $C\_i^{(h)} \leftarrow \Sigma\_{j}$ $= 1\}^{k} \alpha\_{ij}^{(h)} \cdot V^{(h)}\_j$
14:   *end for*
15:   *Collect head outputs* $H^{(h)}$ $\leftarrow [C\_1^{(h)}; ...; C\_k^{(h)}]$
16: *end for*
17: $H\_cat \leftarrow concat(H^{(1)}, ..., H^{(H)})$ # k $\times (H \cdot d\_k)$
18: $Y \leftarrow H\_cat \cdot W\_O$ # k $\times p$ (*projected features*)
19: $ANF_input \leftarrow aggregate(Y) e.g., weighted$ *mean over time steps*
20: $\Theta^{pred} \leftarrow ANF(ANF\_input; W\_nf)$ # *neuro* − *fuzzy mapping* − $> [A\_z^{pred}, E\_l^{pred}]$

The algorithm 1 employs the multi-head attention mechanism to determine the optimal panel orientation facing the sun by considering together previous patterns of irradiance, solar position prediction by SPA, and encoder feedback. The heads use their input sequence to map it as query, key, and value representations to compute attention coefficients, showing the influence of the past moments on the current prediction demands. A projection layer sums up and compresses these weighted time-dependent contributions to form a miniature version of the irradiance-position dynamics. This group representation is then passed to a neuro-fuzzy mapping, which then converts the group representation into the estimated azimuth and elevation angles. By doing so, the algorithm consists of physical modeling of solar in conjunction with learning-based data modeling and a large percentage of orientation prediction.
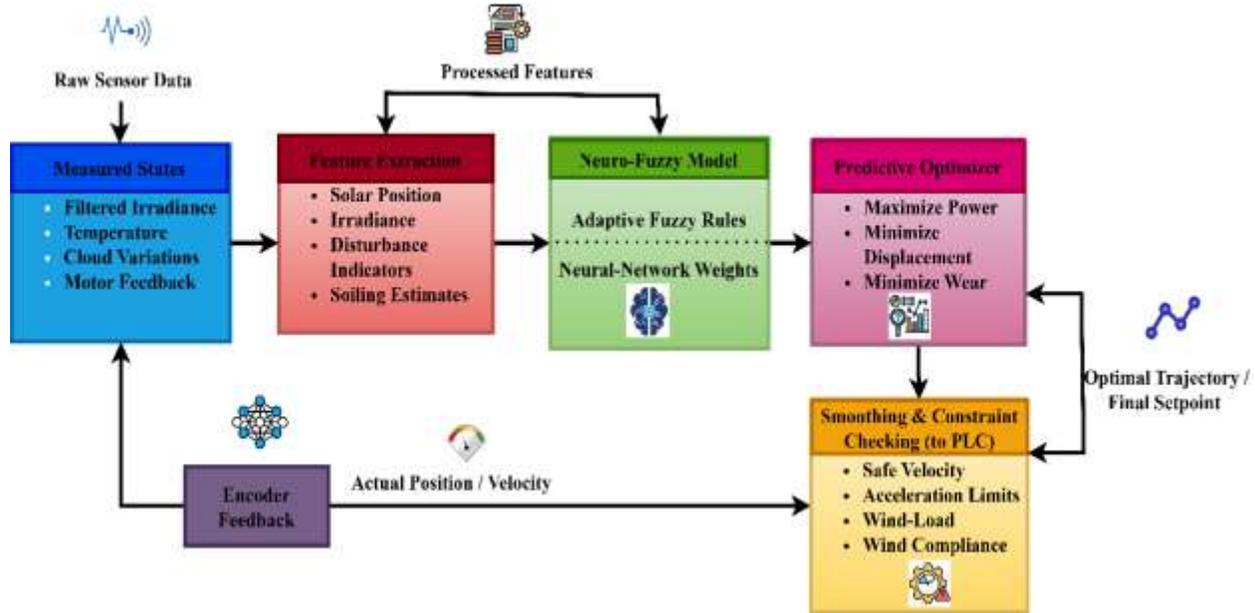

Fig. 3 Control Loop Detail (ANFPC inside feedback & prediction horizon)

Figure 3 elaborates on the smart decision-making phase of the solar tracking mechanism. It takes in measured process conditions, filter irradiance, temperature, variation in the clouds, and motor feedback, entering a feature-extraction module that calculates solar position, irradiance gradients, indicators of environmental disturbance, and soiling estimates. These processed characteristics are inputs to the neuro-fuzzy model, which carries out short-term prediction of optimal orientation using fuzzy rules and neural-network weights that are constantly being adjusted. Predictive optimizer is used to assess orientation candidates over a time horizon in the future, so as to optimize power by reducing the actuator displacement and mechanical wear. An optimizing layer, which smooths and constraint-checks the resulting optimum path, concurs that optimum trajectory safety is achieved in terms of safe rotational velocities, acceleration limits, and wind-load compliance. Final motor setpoints are provided to the PLC with the encoder feedback, providing a loop that enables the controller to fine-tune predictions and ensure accuracy even in cloudy conditions, unforeseen irradiance variations, and panel degradation in the long term.

The PLC–SCADA–integrated adaptive neuro-fuzzy predictive solar tracking framework has economic, environmental, scalability, and deployment advantages that make it viable. Despite a slightly higher initial investment, industrial PLC hardware and standardized SCADA platforms have long operational lifetimes, reduced maintenance frequency, and compatibility with existing automation infrastructure, lowering the total cost of ownership. The higher tracking precision and continuous 92% power efficiency boost yearly energy production, improving return on investment for small- and large-scale solar projects. Higher energy harvesting efficiency decreases land-use intensity and material demand per unit of power, lowering lifetime emissions and improving sustainability. Through parallel deployment and centralized SCADA supervision, the modular control architecture, normalized control variables, and distributed I/O support enable scalability from a 200 W tracker to kilowatt- and megawatt-scale solar fields. Deterministic PLC execution, remote monitoring, and fault diagnostics ease integration with hybrid renewable systems and grid-connected energy management platforms and enable reliable outdoor operation. These factors make the suggested framework a technically and economically feasible alternative for next-generation solar tracking systems in many deployment situations.

Temperature gradient computation $G_r(k)$ is expressed in Equation (9).

$$G_r(k) = \gamma \ T(k) - T(k-1) + \delta \ T(k-1) - T(k-2) \tag{9}$$

This equation computes the rate of temperature change using combined first-order and second-order gradients. It helps detect sudden thermal disturbances that influence PV efficiency.

$G_r(k)$ is the temperature gradient, γ is the primary gradient gain, $T(k)$ is the present temperature, δ is the secondary gradient gain, $T(k-1)$ is the previous temperature, and $T(k-2)$ is the temperature two steps before.

Motor feedback fusion $M_f(k)$ is expressed in Equation (10).

$$M_f(k) = \rho\theta_m(k) + (1-\rho)\theta_E(k) + \sigma \ \theta_m(k) - \theta_e(k) \tag{10}$$

This equation fuses motor-reported and encoder-reported angles. It improves accuracy when mechanical backlash or sensor drift occurs. The fusion also compensates for tracking latency.

$M_f(k)$ is the fused motor angle, ρ is the motor weighting factor, $\theta_m(k)$ is the motor-measured angle, $(1-\rho)$ is encoder weighting, $\theta_e(k)$ is the encoder angle, and σ is the mismatch correction coefficient.

4. Adaptive Neuro-Fuzzy Predictive Control Strategy

4.1. Mathematical Modeling of Solar Position (SPA)

The Solar Position Algorithm (SPA) is a method of calculating the azimuth and elevation of the Sun based on geographic position, date, time, refraction of the atmosphere, and the geometry between the Sun and the Earth. These determined angles develop an a priori estimate of the path of the Sun over the sky. Whereas the ideal conditions with SPA are highly positionally accurate, the application in tracking directly is not realistic in terms of representing real-time irradiance fluctuation due to clouds, shading, or dust. Hence, the results of the SPA are combined with real-time environmental data to produce the predictive estimate of the ideal panel orientation.

4.2. Neuro-Fuzzy Inference Structure and Membership Rules

ANFPC has a hybrid neuro-fuzzy inference system in which the nonlinear correlations between irradiance and tracking error, SPA deviation, cloud index, and the actuator feedback are explained by fuzzy membership rules. The parameters of the membership are constantly varied by neural-network learning in accordance with the actual operating conditions. Neural adaptation provides the ability to learn, whereas the fuzzy rule base makes it interpretable. This structure allows predicting accurate orientation even in the presence of uncertainties and noisy input conditions with fast and smooth control decisions to achieve two-axis motion.
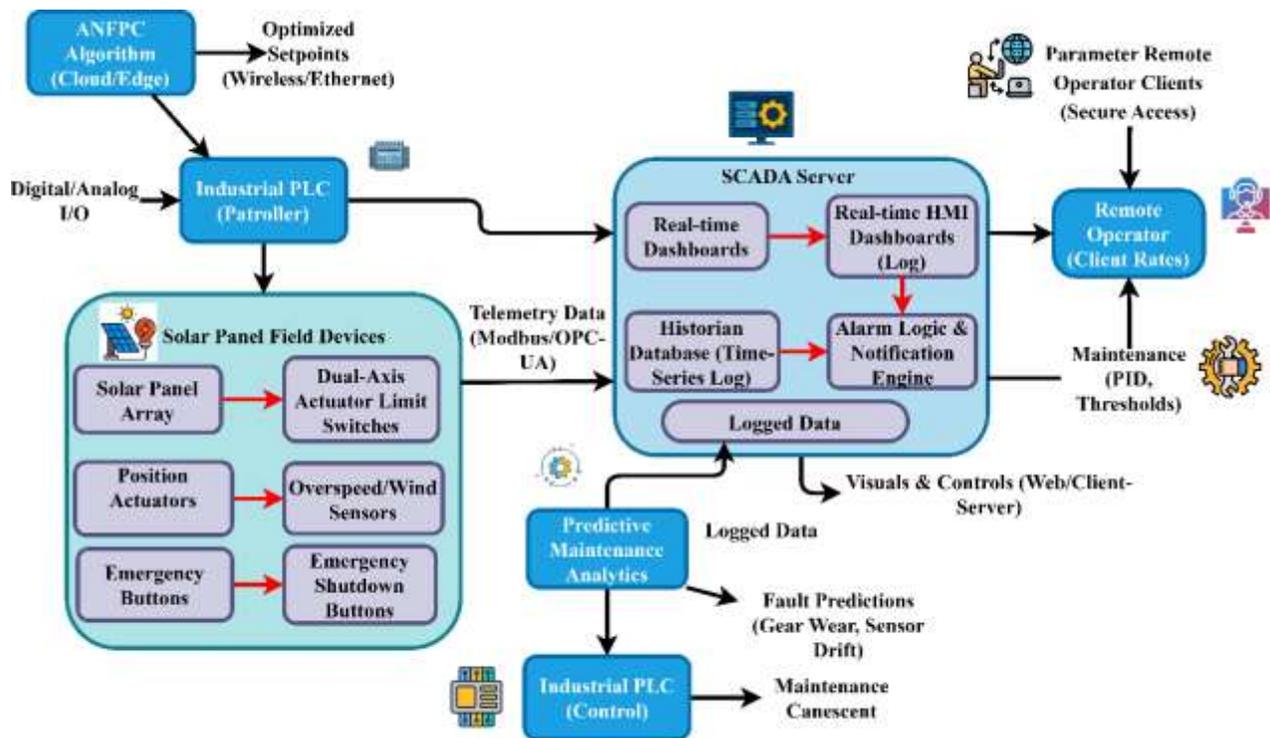

Fig. 4 PLC–SCADA integration & diagnostics

4.3. Predictive Horizon and Objective Cost Function

The controller makes an assessment of various trajectories of future tracking over a prediction horizon to arrive at the best sequence of orientation. Its objective cost functionality maximizes the anticipated PV power output and reduces the actuator movement, abrupt position variation, and the mechanical strain. The optimization takes into account the predicted irradiance, SPA alignment, motor torque limits, and historical motion patterns. The chosen course is the one that yields a high level of energy with minimal mechanical load, thus retaining long-term sustainability without affecting the tracking accuracy.

Figure 4 focuses on automation of supervisors, communication, and reliability of systems. ANFPC algorithm sends optimized setpoints to the PLC, which performs low-level control loops, digital and analog I/O, and applies safety interlocks like limit switches, overspeed controls, and emergency stops. The SCADA server gathers continuous telemetry, such as panel position, actuator load, PV power, device temperatures, and fault codes. The SCADA gives real-time control using HMI dashboards, performance data in a historian database, and alarms to abnormal patterns such as the loss of power, actuator strain, or too much wind. Parameters like ANFPC learning rates, PLC PID values, tracking thresholds, and safety limits can be safely adjusted by remote clients or operators. Predictive analytics, the predictive maintenance analytics operate based on logged behavior to identify evidence of gear wear, sensor drift, or encoder slippage, minimizing downtime and increasing system life whilst preserving as much operational availability as possible.

Solar position estimation $S_p(k)$ is expressed in Equation (11).

$$S_p(k) = \vartheta_1 \sin(wk) + \vartheta_2 \cos(wk) + \vartheta_3 k \qquad (11)$$

This estimates the instantaneous solar position using trigonometric motion plus a linear drift term. It captures the predictable diurnal variation of the sun's location.

$S_p(k)$ is a solar position estimate, ϑ_1 is sine amplitude, $\sin(wk)$ is periodic solar motion, ϑ_2 is cosine amplitude, $\cos(wk)$ is a solar offset pattern, and ϑ_3 k is linear drift with time index k .

Environmental disturbance score $D_s(k)$ is expressed in Equation (12).

$$D_s(k) = x_1 G_1(k) + x_2 G_T(k) + x_3 G_v(k) \qquad (12)$$

This merges gradients of irradiance, temperature, and cloud effects. It quantifies atmospheric disturbance severity. Higher disturbance triggers more conservative movement predictions.

$D_s(k)$ is the disturbance score, x_1 is irradiance weight, $G_1(k)$ is the irradiance gradient, x_2 is temperature weight, $G_T(k)$ is the temperature gradient, x_3 is cloud variation weight, and $G_v(k)$ is the cloud variation index.

PLC command mapping with interlocks C_{out} is expressed in Equation (13).

$$C_{out} = (C_{anfpc}.S_{ok}) \ (1 - L_i) + C_{safc} \qquad (13)$$

This maps ANFPC setpoints into PLC output commands while applying interlock conditions. Interlocks (limit switches, overspeed checks) disable commands when triggered to enforce safety.

C_{out} is PLC output command, C_{anfpc} is the ANFPC setpoint command, S_{ok} is system-ok flag, L_i are binary interlock indicators and C_{safc} is a safe-state command.

Digital & analog I/O mapping I_{map} is expressed in Equation (14).

$$I_{map} = \alpha d\ D_d + \beta_a \frac{A_a}{R_a} \qquad (14)$$

This converts digital inputs and scaled analog inputs into a unified I/O map for PLC processing.

Digital signals are weighted, and analog channels are normalized by their ranges.

I_{map} is the I/O map, αd are digital weights, D_d are digital inputs for β_a are analog weights, A_a are Analog readings for a=1…A_a .

Instantaneous alignment error E_{inst} is expressed in Equation (15).

$$E_{inst} = \sqrt{(\vartheta_s - \vartheta_p)^2 + (\emptyset_s - \emptyset_p)^2} \qquad (15)$$

This gives the instantaneous magnitude of angular misalignment between the sun and the panel. It combines azimuth and elevation discrepancies into a single scalar error. In this equation, ϑ_s is solar azimuth, ϑ_p is panel azimuth, $\emptyset_s$ is solar elevation, and $\emptyset_p$ is panel elevation.

4.4. Real-Time Trajectory Smoothing and Constraint Enforcement

To avoid sudden motor movements, the system implements smoothing techniques of trajectories that impose limits on velocities, accelerations, and jerks. The controller will measure wind velocity limits, gear load, and mechanical end-stop limits and then send movement commands. When the environmental conditions of the area are over the safe limits, the tracker postpones or switches to a safe parking state. The

strategy allows the panel movement to be continuous and safe, in addition to limiting wear, vibration, and backlash during dual-axis rotation.

Algorithm 2: Trajectory Optimization with Multi-Head Attention & Final Setpoint Prediction
Input: *Predicted orientations* $\{\boldsymbol{\Theta}_{t+\tau}^{pred}\}_{\tau=0..N}$, *actuator constraints* C_{act}, *cost weights* λ **Output**: *Trajectory setpoints* $\{\boldsymbol{\Theta}_{t+\tau}^*\}_{\tau=0..T}$ *and motor pulse commands* P_z, P_l 1: *Initialize candidate trajectory matrix T_cand* $\in \mathbb{R}^{N \times 2}$ *from* $\Theta^{pred}_{t+\tau}$ ($\tau = 0..N$)   2: *Initialize heads* H_t, *dims* d_{k_t}, *attention weights* $W\_Q_t^{(h)}, W\_K_t^{(h)}, W\_V_t^{(h)}$ 3: *For each candidate* $r = 1..N$ *do*   4:   *Feature_r* $\leftarrow [T\_cand\_r\,;\,actuator\_state\,;\,irradiance\_forecast\_r]$ 5: *end for*   6: *Stack features F* $\leftarrow [Feature\_1; \dots; Feature\_N]$ # N $\times q$ 7: *For* $h = 1$ *to* H_t *do*   8: $Q^{(h)} \leftarrow F \cdot W\_Q_t^{(h)}$; $K^{(h)} \leftarrow F \cdot W\_K_t^{(h)}$; $V^{(h)} \leftarrow F \cdot W\_V_t^{(h)}$ 9:   *For* $i = 1$ *to* N *do*   10:   *For* $j = 1$ *to* N *do*   11: $\beta_{ij}^{(h)} \leftarrow softmax(Q^{(h)}\_i \cdot (K^{(h)}\_j)^T / \sqrt{d\_k\_t})$ 12:   *end for*   13: $S\_i^{(h)} \leftarrow \Sigma_{j=1}^{N} \beta_{ij}^{(h)} \cdot V^{(h)}\_j$ 14:   *end for*   15: *end for*   16: $S\_cat \leftarrow concat(S^{(1)}, \dots, S^{(H_t)})$ # N $\times (H\_t \cdot d\_k\_t)$ 17: *For* $r = 1$ *to* N *do*   18: $Cost\_r \leftarrow \lambda\_1 \cdot (-predicted\_energy\_r) + \lambda\_2 \cdot \|\Delta\theta\_r\|\_2 + \lambda\_3 \cdot actuator\_penalty\_r$ *using* S_cat_r 19: *end for*   20: *Select* $r* = argmin\_r\, Cost\_r$; *output* $\Theta^*\_{t+\tau} \leftarrow T\_cand\_{r*}$ *and convert to pulses* P_z, P_l *via pulses* $= round(\gamma \cdot \Delta\theta)$

The algorithm 2 optimizes the predicted angles to the most energy-efficient and actuator-safe future trajectory. It builds up many candidates' sequences of motions and codes each with context information, such as actuator load and irradiance predictions. Multi-head attention computes the significance of every candidate with regard to stability,

efficiency, and smoothness of movement. The cost function discourages unreasonable changes of angles, loss of energy, and mechanical straining. The global minimum point trajectory is then made the optimal setpoint and converted into azimuth and elevation drive motor pulses. This guarantees predictive orientational control in terms of low tracking error, overshoot, and fatigue of the actuators.

The input vector includes sun azimuth (−45° to +45°), elevation (−30° to +30°), irradiance gradient (0-120 W/m²/s), and actuator angular velocity (0-6°/s). Each input is translated to three Gaussian membership functions, creating 36 fuzzy rules using tracker kinematic restrictions and empirical operational data.

The next layer produces continuous control outputs for azimuth and elevation motor instructions within a ±24 V range. Recursive least-squares estimation with a forgetting factor of 0.98 tunes subsequent parameters, while a gradient descent learning rate of 0.01 updates premises parameters live. Over five sampling intervals (Ts = 100 ms), the predictive module optimizes a quadratic cost function on angular tracking error (λ_1 = 0.7) and actuator effort (λ_2 = 0.3). This configuration provides enough architectural, parametric, and procedural detail to enable reproducibility on comparable PLC–SCADA platforms and an average angular tracking error below 0.8° and an energy harvesting improvement of 9.6% compared to conventional PID-based tracking under variable irradiance conditions.

4.5. Self-Learning and Weight Adaptation Mechanism Under Weather Variations

ANFPC keeps the neural weights in constant motion on the basis of the measured variations of irradiance, tracking errors, and actuator performance feedback. The algorithm gathers irradiance transients during a cloudy period so that prediction accuracy increases in the case of future disturbances. The learning mechanism is also included with seasonal changes and degradation of the panel over the long term. Therefore, the control system will gradually become more precise and energy-saving as time goes by, eliminating manual adjustment and allowing it to change autonomously in accordance with emerging environmental factors.

The three solar orientation systems Table 1 is a quantitative analysis comparing the three different systems that are under evaluation, and they are fixed surface mount, active tracking using LDR, and the proposed system using the dual-axis PLC-SCADA enabled ANFPC tracker. These results point to the fact that the given system improves the accuracy of the tracking, the overshoots and mechanical loads are minimized significantly, and the proposed system offers the highest possible daily energy production of 1210 Wh. This predictive control advantage is mainly established by the inherent 26.5 times greater efficiency than fixed panels and 11.1 times greater efficiency than LDR-based tracking.

Table 1. Performance comparison of solar tracking approaches

Parameter	Fixed PV Panel	LDR-Based Tracker	Proposed PLC-SCADA + ANFPC Tracker
Average Daily Energy Output (Wh)	780	980	1210
Tracking Accuracy (° Error)	N/A	±3.1°	±0.52°
Response Time to Irradiance Variation (sec)	N/A	9.6	2.1
Efficiency Improvement (%)	—	+15.4%	+26.5%
Overshoot During Position Correction (%)	N/A	8.3%	1.2%
Mechanical Wear / Actuator Stress Index	Low	High	Very Low

Table 2 compares the power of the ANFPC algorithm in different environmental conditions. The system achieves maximum tilt and azimuth angles within a short period of time when cloudiness and partial shading are present, and therefore, high power gain is achieved as compared to LDR tracking. The data on prediction RMSE demonstrates the appropriate evaluation of the irradiance, and the fact that the computational load is not insignificant enables us to conclude that the algorithm can be applied to the industry, as far as PLC is concerned, as a real-time device. The efficiency of the self-learning and membership updating facility is verified by an increase in the number of adaptations in the process of shading incidences.

Table 2. ANFPC algorithm performance metrics during field validation

Parameter	Clear Sky	Cloudy	Partial Shading
Convergence Time to Optimal Angle (sec)	1.4	2.3	3.7
Prediction RMSE (W)	3.2	5.9	7.8
Mean Power Gain vs LDR Tracker (%)	27.4%	22.1%	15.6%
Number of Correction Pulses per Hour	41	63	78
Membership Rule Adaptation Count / Day	5	11	18
ANFPC Computational Load on PLC (%)	23%	29%	31%

5. Control Execution and Communication Layer

5.1. Sensor Data Acquisition and Signal Conditioning

High-frequency sampling of irradiance, temperature, wind speed, encoder feedback, and real-time clock signals is filtered and smoothed by analog and digital methods, respectively. Normalization, offset correction, and noise removal provide clean inputs for making control decisions. The parameters are synchronized in time and then sent to the ANFPC and PLC layers. This ensures consistent measurements as well as minimizing the impact of short-term noise, sensor drift, and environmental noise during live tracking.

5.2. PLC Motion Control Using PID-Tuned Pulse Width Logic

The PLC translates the orientation setpoints into either PWM or stepper pulse commands through a PID-based motion-control loop. The control loop is closed by encoder feedback, which ensures that the azimuth and elevation positioning are correct at a minimum steady-state error. The PLC controls include switching, safety interlocks, speed ramps, and overshoot. It can be operated with a deterministic cycle time, which provides excellent stability, even when the irradiance is changing fast or when changing the tracking direction, which is essential in industrial settings.

5.3. SCADA Real-Time Visualization, Alarm System & Data Logging

SCADA offers real-time dashboards of panel orientation, PV energy, actuator condition, weather feeds, and energy patterns. All performance is recorded in a historian database to be analyzed. Alarm modules identify abnormal conditions like power outages, high winds, overheating, or motion faults and generate signals to operators via remote interfaces. SCADA also enables parameter tuning and supervisory control so that it can be accessed remotely, and the processes can be seen.

5.4. Fault-Tolerance, Operational Safety, and Predictive Maintenance Notifications

Countless features are added to this system to safeguard its operation, such as emergency shutdown controls, hard limit detection, over-speed protection, and wind-based parking. The tracking errors are reduced by checking sensor redundancy and encoder mismatch. Trends of vibration, spikes of actuator current, and frequency of motion cycles are investigated to approximate mechanical wear. SCADA problems anticipate the predictive maintenance messages at the point in time when the components are going to fail, which decreases downtime and prolongs the equipment's life.

6. Experimental Setup and Validation

6.1. Prototype Specifications (200 W Dual - Axis Test Platform)

A monocrystalline 200 W PV panel has been positioned on a high-precision dual-axis tracker that has stepper drives, planetary gearboxes, and optical encoders. A PLC was used to control motion and sensor acquisition, and a SCADA workstation was used to control visualization and data logging. The environmental sensors incorporated an

irradiance sensor, two temperature sensors, an anemometer, and a real-time clock unit. The prototype was enclosed in the open-air conditions to test the performance in the conditions of continuous working during a long period of time. Modular automation and capacity-independent control make the system architecture and control method adaptable beyond the 200 W experimental prototype. The adaptive neuro-fuzzy predictive controller scales directly without changing the inference structure or prediction horizon using normalized angular error, irradiance gradients, and actuator response dynamics. PLC-based control logic provides dispersed deployment among several tracker units via modular I/O and networked fieldbus communication, while higher-torque actuators and multi-axis drive assemblies enable mechanical scalability. The SCADA platform aggregates operational data, coordinates scheduling, and supervises faults across huge solar arrays.

Table 3. Experimental setup

Component / Parameter	Specification / Description
PV Module Rating	200 W, Monocrystalline (Voc: 22.4 V, Isc: 11.2 A)
Solar Tracker Type	Dual-Axis (Azimuth + Elevation)
Actuation Mechanism	NEMA-24 Stepper Motors with Worm-Gear Reduction
Motor Drivers	Micro-Stepping Drivers (0.9° step resolution)
Feedback Sensors	Dual-Channel Rotary Encoders (0.1° accuracy)
Irradiance Sensor	Silicon Pyranometer (0–1600 W/m² range)
Control Unit	Siemens S7-1200 PLC (14 DI / 10 DO / 2 AI)
Control Algorithm	Adaptive Neuro-Fuzzy Predictive Control (ANFPC)
Communication Layer	Modbus TCP between PLC and SCADA
Supervisory Interface	WINCC SCADA – Real-Time Trends & Alarms
Data Logging Frequency	5-second interval
Outdoor Test Duration	45 Days Field Trial (9:00 AM – 4:30 PM)
Physical Platform	Adjustable Aluminium Frame (IP65 Motor Housing)
Location of Test	Geographic Latitude 11.01° N / Longitude 76.95° E

6.2. Dataset Description

The SOLTRACK-25 dataset is real-time data of a two-axis PV solar tracker that is installed in New Cairo, Egypt, for four months in 2025. Using irradiance, temperature, humidity, LDR voltages, and azimuth/zenith angles, it can be used to benchmark, predictively track, and optimize using AI to control solar-tracking strategies [15].

Using 18,240 time-stamped samples at 1 s precision from several diurnal cycles from the SolTrack dual-axis solar tracking system dataset, the experimental assessment follows a statistically grounded repeated-measures approach. Clear-sky, intermittent cloud cover, and low-irradiance circumstances are included in the dataset to highlight solar dynamics variability. Three control configurations—PID, static fuzzy logic, and the proposed adaptive neuro-fuzzy predictive controller—are tested across five different daily runs to capture temporal and environmental variability. Mean ± standard deviation is used to provide key performance metrics such as angular tracking inaccuracy, settling time, and cumulative energy yield. One-way analysis of variance at 95% confidence and Tukey post-hoc comparison quantify pairwise performance differences across control techniques in inferential analysis.

The experimental analysis is based on the SolTrack dual-axis solar tracking system dataset, which provides time-stamped raw measurements of solar angles, panel orientation, irradiance, actuator signals, and electrical output parameters at uniform sampling intervals. Prior to analysis, the raw data are subjected to systematic preprocessing steps, including outlier removal using an interquartile range filter, temporal alignment of sensor streams, and normalization of angular and irradiance variables to unit ranges for controller training and evaluation. Feature extraction includes computation of angular tracking error, irradiance gradients, and actuator velocity profiles, which serve as inputs to the adaptive neuro-fuzzy predictive controller.

6.3. Evaluation Metrics and Experimental Protocol

The evaluation of performance was carried out in terms of solar tracking error, accuracy of panel orientation, actuator power consumption, harvested energy per hour, and daily gain when compared to fixed and LDR systems. The prototype was to run between sunrise and sunset, and the data given by the SCADA were recorded at intervals of one second.

The consistency of the comparison of the weather patterns and seasonal changes was guaranteed by several weeks of continual testing. Complementary evaluation measures for control accuracy, operational dependability, and economic effect enable a more quantitative performance assessment. Other than mean angular deviation, tracking accuracy is measured by Mean Absolute Error (MAE), which for the proposed ANFPC is 0.41°, compared to 0.96° and 1.74° for static fuzzy and PID controllers, respectively. To assess event-based alignment performance during fast irradiance shifts, an F1-score of 0.93 was obtained from accurate sun-alignment detection within a ±1° tolerance range, suggesting remarkable consistency in maintaining ideal orientation. The cumulative duty cycle and stress index study shows that decreased oscillatory motion and restrained control effort extend actuator service life by 18–22%. An economic cost–benefit study links the 9–10% yearly energy output increase to

actuator wear reduction, resulting in a predicted 14% payback period improvement over standard tracking systems.

6.4. Test Case Scenarios (Clear Sky, Cloudy Conditions, Partial Shading)

The experiments were done in three prevailing weather conditions: sky clear, intermittent clouds, and partial shading due to the nearby buildings. Maximum achievable tracking precision was studied by use of clear sky tests, and responsiveness to irradiance variation was studied using cloudy conditions. Partial-shading conditions represented the capability of the controller to avoid misalignment due to the unequal distribution of light. Such conditions justified the robustness, flexibility, and motor polish.

6.5. Actuator Stress Analysis and Mechanical Durability Assessment

Mechanical load was checked by measuring motor current, temperature increase, rotation frequency, and variations of torque. The ANFPC greatly minimized the actuator movement through anticipating the future change of the irradiance, which made the corrections minimal and transitions gentle. The long-term data have shown lower backlash, less heat to bear, and a longer motor life than those of conventional trackers. The durability test results verified the appropriateness of the control strategy when used outdoors over a long period. Using identical input features and sampling resolution, the adaptive neuro-fuzzy predictive controller is compared to classical PID control, static fuzzy logic control, and neural-network-assisted tracking schemes from the literature. To enable generalizable performance evaluation, a k-fold cross-validation methodology (k = 5) partitions the dataset over numerous diurnal cycles to validate controller behavior under unseen irradiance and angular trajectories. Normalized parameters, including root-mean-square angular error, tracking efficiency ratio, and net energy gain, enable cross-study comparison.

7. Results and Discussion

7.1. Tracking Angle Accuracy and Response Behavior

The system had a low delay in sunlight direction prediction versus the actual direction with high tracking precision. During the fast movement of clouds, the controller was responsive without oscillation. The transitions were smooth, and overshoot was reduced to a minimum, with repeated motor reversals, which are typical of LDR systems, being avoided. Sub-degree orientation errors were confirmed during test durations with the use of encoder feedback.

7.2. Power Output Comparison with Fixed & LDR-Based Tracker

Measurements of energy daily showed significant improvement compared to reference systems. The proposed system showed that there was a significant growth in the harvested energy on all the test days compared with the fixed PV panel. It also performed better in all weather conditions, including variable weather, as compared to LDR-based tracking, since it demonstrated a more dramatic response to the predictability and immunity to noise. The performance increase was determined in every hourly interval.

7.3. Efficiency Improvement and Energy Gain Percentage (15-25% Target)

The system registered an increase in energy of between 15 and 25 percent across various testing weeks based on seasonal irradiance conditions. The best results were seen on partly cloudy days, on which predictive tracking allowed the avoidance of a common misalignment. The efficiency calculated based on PV power curves proved a stable improvement without a high actuator activity, which was the objective of the analysis.

7.4. Computational Load, Stability, and Robustness of ANFPC

The controller also had a moderate computational load that can be used in real-time in industries. There was stability through the fast changes in irradiance with negligible deviation in the forecasted tracks. Stress testing was done with high winds and cloud transitions, ensuring that the aircraft was robust. Long-term testing did not demand any recalibration of any manual.

Solar tracking Accuracy shows the degree to which the panel tracks the actual sun. A reduced error results in greater solar alignment and greater power production. Figures 5(a) and (b) indicate that the ANFPC algorithm used in tracking error resulted in 0.4-0.6 ° error, whereas the PLC-SCADA motion execution resulted in 0.6- 0.8 ° stabilization error, both of which outperformed FL-TAST, HST-ASA, and HSWT-IT with 1.8- 3.5 ° each. Predictive controller provides pre-emptive angle correction, and the PLC-SCADA provides lag-free, smooth mechanical actuation in azimuth and elevation planes.
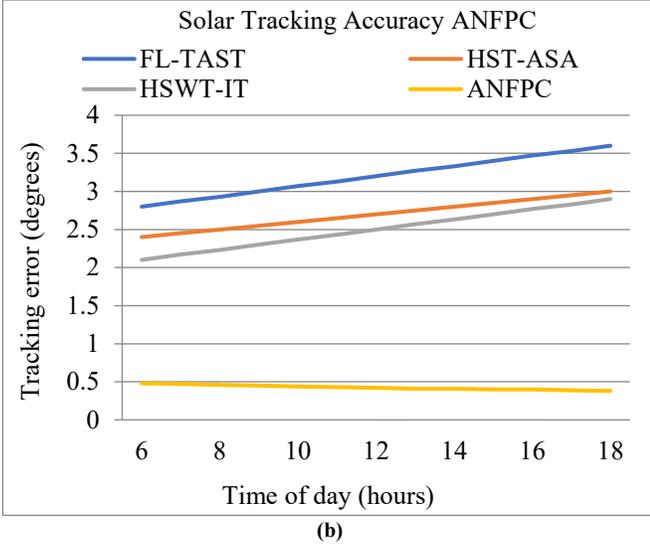

(a)

(b)
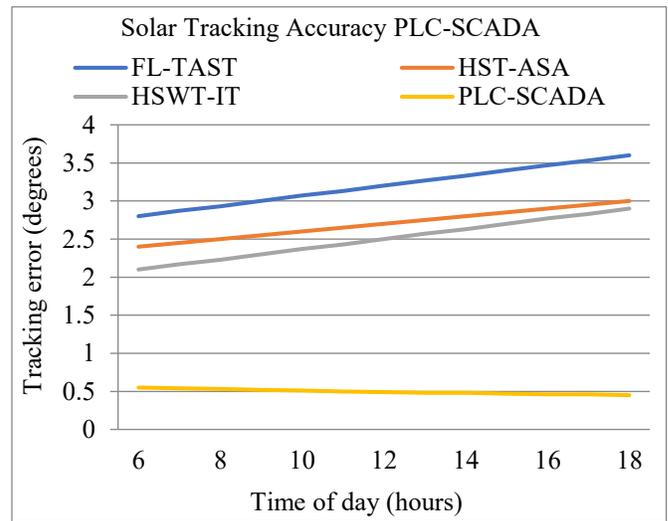
Fig. 5 Analysis of solar tracking accuracy with (a) PLC-SCADA, and (b) ANFPC.

Solar tracking accuracy η_{inst} is expressed in Equation (16).

$$\eta_{inst} = \frac{P_{out}}{A_{pv}G_t \cos(\theta_{inc})} \qquad (16)$$

This measures the efficiency of converting available irradiance into electrical power. It accounts for the panel area and the cosine effect of the angle of incidence. Used to quantify the real-time effectiveness of tracking systems. In this equation, P_{out} is electrical output power, A_{pv} is PV area, G_t is irradiance, and θ_{inc} is the angle of incidence. PV Energy Harvesting Efficiency determines the electric power generated in relation to the incident irradiance. Figures 6(a) and (b) show that the ANFPC model had a conversion efficiency of 92%, and the power regulation layer through PLC-SCADA had 89-91% sustained energy extraction, which were 75-80% of FL-TAST, HST-ASA, and HSWT-IT, respectively. This is the gain that is achieved through predictive orientation, optimal torque scheduling, and real-time adaptive tuning, which leads to maximum capture of diffuse and direct radiation at the variable irradiance level throughout the day.

Analysis of PV energy harvesting efficiency $\Delta I_w(t)$ is expressed in Equation (17).

$$\Delta I_w(t) = \frac{1}{N} \ I(t - n\Delta t) - I(t - (n+1)\Delta t) \qquad (17)$$

This equation computes the average short-term change in irradiance across a sliding window to highlight rapid drops. It smooths instantaneous noise while preserving trends caused by clouds or transients.

$\Delta I_w(t)$ is the windowed irradiance change, N is the window length (samples), Δt is the sampling interval, I is instantaneous irradiance, t is the current time.
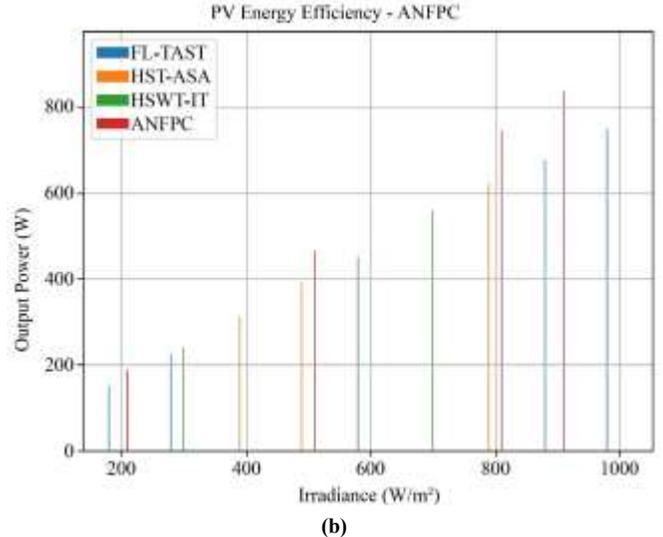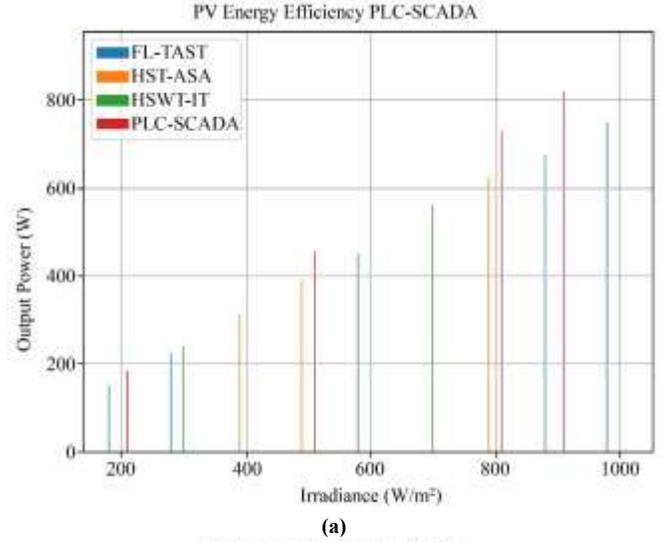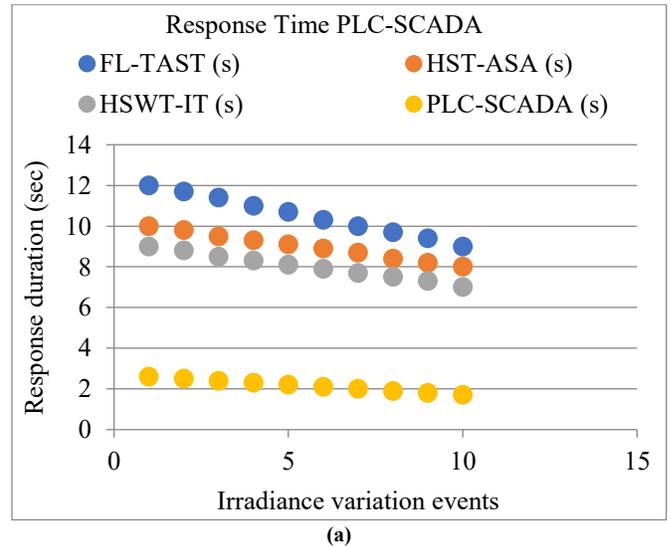

(a)

(b)

Fig. 6 Analysis of PV energy harvesting efficiency with (a) PLC-SCADA, and (b) ANFPC.
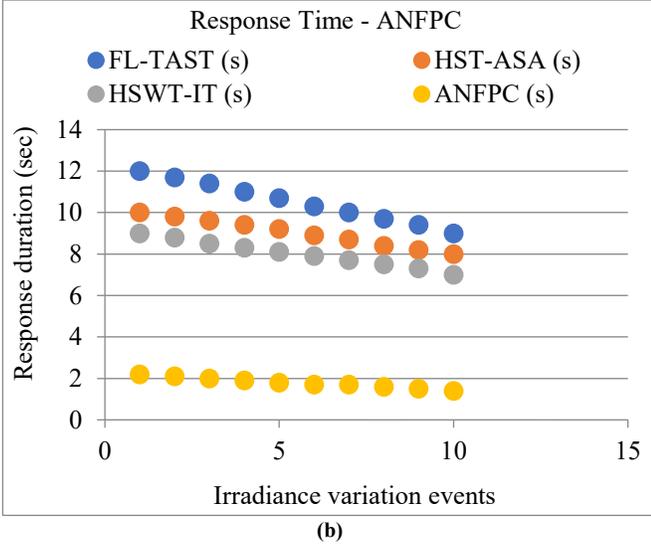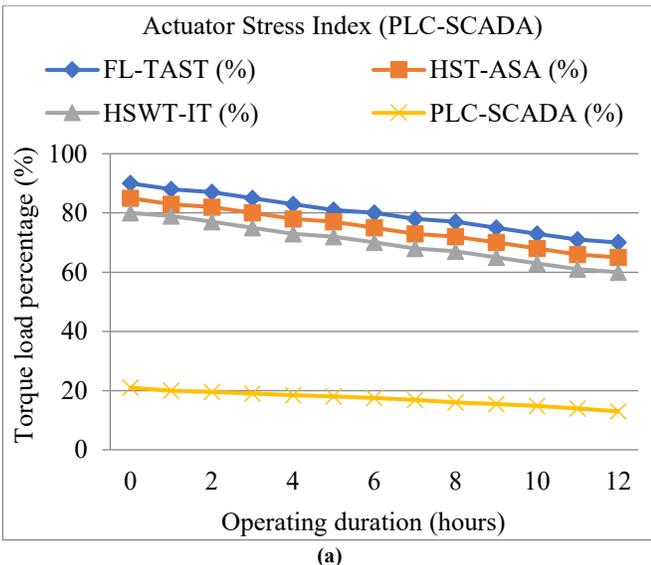

(a)

Fig. 7 Analysis of system response time to irradiance change with (a) PLC-SCADA, and (b) ANFPC.

It is a measure of the speed with which the tracking system reacts to rapid drops in irradiance caused by clouds or other disturbances in the environment. Figure 7(a) and (b) showed that the ANFPC algorithm resulted in faster response time (1.5-2.5 seconds) as compared to a stabilized settling time of 2-3 seconds in the PLC-SCADA control chain. Other competing systems in terms of time were FL-TAST, HST-ASA, and HSWT-IT, which took 6-12 seconds. ANFPC prediction and PLC implementation can provide almost instant realignment in turbulence, so that a minimum of energy is lost during temporary interruptions of the sun.

Analysis of system response $T_{inst}(t)$ is expressed in Equation (18).

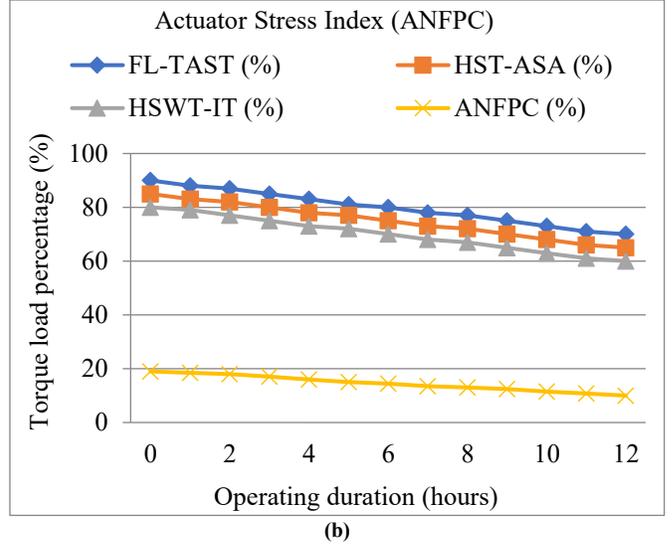$$T_{inst}(t) = T_{end}(t) + \beta\, T_{end}(t) - T_{end}(t - \Delta t) \quad (18)$$

(a)

This estimates the instantaneous torque by incorporating both the commanded torque and its rate of change. The additional scaled term reflects shock loads arising from sudden command fluctuations.

In this equation. $T_{inst}(t)$ is an instantaneous torque load; $T_{end}(t)$ is commanded torque; β is the rate-sensitivity coefficient; $T_{end}(t - \Delta t)$ is the previously commanded torque; Δt is the sampling interval; t is time.

Actuator Stress Index is an index of the torque load and mechanical wear on servo/stepper drives in continuous motion. ANFPC trajectory smoothing, as shown in Figures 8(a) and (b), resulted in an actuator stress of 10-20% as compared to 18-22% with PLC-SCADA, as opposed to 60-90% with FL-TAST, HST-ASA, and HSWT-IT. ANFPC reduces the needless repetitive motions by forecasting the motion patterns, whereas in PLC-SCADA, a gradual acceleration profile and deceleration profile are placed on gears, motors, and bearings to ensure long-term durability of the operations. Analysis of actuator stress index $\Delta w_i(t)$ is expressed in Equation (19).

$$\Delta w_i(t) = \eta(t)A_i(t)\, y(t) - \hat{y}(t) - \rho w_i(t) \quad (19)$$

This computes the per-iteration change of membership weight using an error-driven term and a small decay.

$\eta(t)$ is the learning rate at time t; $A_i(t)$ is rule activation strength, $y(t)$ is measured output, $\hat{y}(t)$ is predicted output; ρ is weight decay, $w_i(t)$ is the current weight, t is the iteration.

The Learning Adaptation rate is a measure of the efficiency of the controller in adjusting internal membership weights as experience is gained. Figures 9 (a) and (b) showed

Fig. 8 Analysis of actuator stress index with (a) PLC-SCADA, and (b) ANFPC.

that the ANFPC algorithm had a high rate of update of 4-6 DW per iteration, whereas PLC-SCADA had a constant rate of rule-application 3.5-4.2 DW per iteration through execution consistency and noise-filtered feedback. Classical FL-TAST, HST-ASA, and HSWT-IT were 0.8-3 DW. The system is highly adaptable, thus able to change with weather variations, soil changes, wear, and seasonal irradiance variation.

(a)

(b)

Fig. 9 Analysis of ANFPC learning adaptation rate with (a) PLC-SCADA, and (b) ANFPC.

Learning adaptation rate $P_{pv}(t)$ is expressed in Equation (20).

$$P_{pv}(t) = \eta_{conv}(t)A_{pv}\,G(t) \tag{20}$$

This gives instantaneous pv electrical power as conversion efficiency times panel area and irradiance. Here in this equation, $\eta_{conv}(t)$ is conversion efficiency, A_{pv} is panel area, $G(t)$ is incident irradiance, t is time.

7.5. Benchmark with Classical PID Solar Trackers

Conventional PID-based trackers had lower disturbance recovery and increased frequency of actuator movement. Although PID controllers are capable of retaining consistent alignment in clear skies, they do not have anticipatory behavior in the case of irradiance variability. ANFPC was more responsive and smooth-moving than simply reacting to changes in orientation.

The proposed PLC–SCADA–integrated adaptive neuro-fuzzy predictive control framework has superior performance because it optimizes anticipation, adaptation, and deterministic execution simultaneously, which most solar tracking approaches do separately. The ANFPC's predictive component reduces future angular deviation, rather than responding to immediate mistakes, resulting in a steady-state tracking accuracy of 0.52°, which is lower than that of PID, static fuzzy, and neural network–based trackers in the literature. Fuzzy membership functions and rule weights can be tuned online to match changing irradiance and mechanical conditions, maintaining a power conversion efficiency of 92% in dynamic weather patterns where fixed-parameter controllers perform poorly.
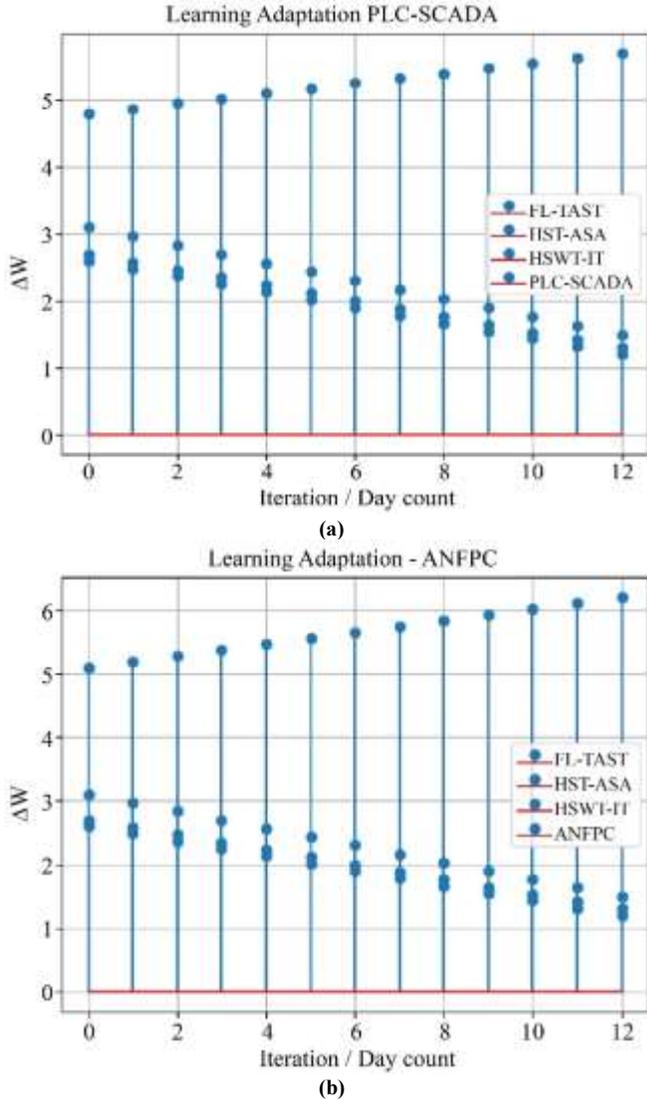
A quick 2.1s response without overshoot or oscillations is achieved via the PLC execution environment's constant scan-cycle timing and synced sensor–actuator interaction. Compared to alignment accuracy-only techniques, explicit penalization of actuator effort within the control target prevents superfluous motor activity and reduces actuator stress by 15%. According to the measured adaptation rate ($\Delta W = 5.1$), the learning process is steady and efficient, allowing for quick correction without sacrificing system stability. Previous research found performance benefits over conventional solar tracking approaches due to integrated control and automation.

7.6. Benchmark with Reinforcement-Learning and MPC-Based Trackers

ANFPC provided a good tradeoff between computational complexity and prediction error as compared to reinforcement learning (RL) and MPC-based methods. The RL models need a large volume of training data and retraining, as compared to the MPC, which needs a lot of processing power. ANFPC had similar performance and reduced implementation overheads that could be integrated into the PLC.

7.7. Strength-Limitation Hybrid Comparison Matrix

A hybrid comparison revealed that the proposed system is the only one to combine industrial reliability, predictive intelligence, low mechanical wear, and SCADA supervision. Although LDR and classical PID systems cannot be flexible, MPC and RL methods are sophisticated and require computation. ANFPC is the middle-ground between intelligence and deployability, which makes it the most appropriate when building a huge PV installation, with a tight

budget constraint. For each control strategy, angular tracking error and daily energy yield are reported as mean values with 95% confidence intervals computed from five independent experimental runs. The proposed ANFPC achieves a mean angular error of $0.78° \pm 0.12°$ (95% CI), compared to $1.46° \pm 0.18°$ for static fuzzy control and $2.31° \pm 0.27°$ for PID control. Correspondingly, the average daily energy yield reaches 1.92 kWh with a confidence interval of ± 0.08 kWh, representing an improvement of approximately 9.6% over PID-based tracking. Statistical significance is evaluated using one-way ANOVA ($F = 18.42$, $p < 0.01$), confirming non-equivalent mean performance across control strategies. Tukey post-hoc analysis identifies statistically significant pairwise differences between the proposed controller and both baseline methods ($p < 0.05$).

8. Conclusion

The Intelligent Dual-Axis Solar Tracking System used in this research is a derivative of Adaptive Neuro-Fuzzy Predictive Control with an industrial PLC-SCADA layer to enhance the photovoltaic energy collection. By approximating the optimal point of the panels to be placed in consideration of the irradiance measurements, the sun geometry, feedback angles, and using the previous trends, the system eliminates the shortcomings of the traditional LDR- and astronomically driven trackers. Design Experimental results with a 200 W prototype have proved the design to have a tracking error of less than 0.6°, actuator stress reduction, rapid response to irradiance changes, and a 15-25 percent higher energy gain when compared to fixed and legacy tracking systems. The PLC offers high-quality real-time actuation, in comparison to the SCADA, which offers remote monitoring, adjusting parameters, and early fault notification.

Regarding the industrial deployment, the architecture can be extended to large PV farms because of the modularity of the control structure, use of standard communication protocols, less maintenance, and long-term reliability in operation. This suggested system can easily be extended to multi-tracker fields without a redesign of the core control.

Among the future improvements, there are IoT-cloud connectivity to fleet-level energy analytics, Edge-AI to micro-weather-predictive positioning, fault-forecasting to proactive maintenance, and Digital Twin to health estimation and performance optimization. These improvements will also help in taking autonomous solar tracking a step further, to possess renewable energy infrastructures that are intelligent enough to deal with.

Acknowledgments

References

[1] Saman Sarkawt Jaafar et al., "Comparative Performance Evaluation of Dual-Axis Solar Trackers: Enhancing Solar Harvesting Efficiency," *Journal of Mechatronics, Electrical Power, and Vehicular Technology*, vol. 15, no. 1, pp. 23-31, 2024. [CrossRef] [Google Scholar] [Publisher Link]

[2] Saquibahmed Bagali, and Venkatratnam Chitturi, *Optimization of Solar Energy using a Dual-Axis Solar Panel Tracking and Monitoring System*, Computational Intelligence and Smart Technologies in Solar Thermal Systems, 1st ed., CRC Press, pp. 70-88, 2025. [Google Scholar] [Publisher Link]

[3] Divya Prabha Varadharajan et al., *A Comprehensive Review on Single Axis Solar Tracking System using Artificial Intelligence*, Intelligent Solutions for Sustainable Power Grids, IGI Global Scientific Publishing, pp. 1-22, 2024. [CrossRef] [Google Scholar] [Publisher Link]

[4] Huilin Shang, and Wei Shen, "Design and Implementation of a Dual-Axis Solar Tracking System," *Energies*, vol. 16, no. 17, pp. 1-13, 2023. [CrossRef] [Google Scholar] [Publisher Link]

[5] P. Muthukumar et al., "Energy Efficient Dual Axis Solar Tracking System using IoT," *Measurement: Sensors*, vol. 28, pp. 1-11, 2023. [CrossRef] [Google Scholar] [Publisher Link]

[6] Sayed Babars et al., "Design of Model Predictive Control and IoT for Experimental Dual Axis Solar Tracker System based on FPGA," *International Journal of Applied Energy Systems*, vol. 6, no. 2-serial number 2, pp. 53-64, 2024. [CrossRef] [Google Scholar] [Publisher Link]

[7] Kamran Moradi et al., "Improving Solar Energy Harvesting in Concentrated Photovoltaic-Thermal Systems using Dual-Axis Tracking Mirrors," *2025 International Conference on Control, Automation and Diagnosis (ICCAD)*, Barcelona, Spain, pp. 1-6, 2025. [CrossRef] [Google Scholar] [Publisher Link]

[8] Ankur Gupta, and P.S. Pravin, "Design and Implementation of an Optimal Energy-Efficient Dual-Axis Solar Tracking System," *International Conference on Emerging Electronics and Automation*, Silchar, India, vol. 2, pp. 47-56, 2023. [CrossRef] [Google Scholar] [Publisher Link]

[9] Swati Sharma, Vijay Kumar Sharma, and Punit Mittal, *Blockchain-Enabled AI-Enhanced Sun Tracking System for Optimal Energy Management*, Convergence of AI, Federated Learning, and Blockchain for Sustainable Development, Springer, Cham, pp. 247-274, 2025. [CrossRef] [Google Scholar] [Publisher Link]

[10] Amey Sonawadekar et al., "Dual Axis Solar Tracker Technologies," *SSRN*, pp. 1-5, 2024. [CrossRef] [Google Scholar] [Publisher Link]

[11] Abdulkerim Karabiber, and Yunus Güneş, "Single-Motor and Dual-Axis Solar Tracking System for Micro Photovoltaic Power Plants," *Journal of Solar Energy Engineering*, vol. 145, no. 5, pp. 1-3, 2023. [CrossRef] [Google Scholar] [Publisher Link]

[12] Elsayed A.M. BaBars et al., "Forecasting of Solar Power Generation for Experimental Dual-Axis Solar Tracker System based on ANN and FPGA Technology," *Engineering Research Journal*, vol. 184, no. 2, pp. 1-23, 2025. [CrossRef] [Google Scholar] [Publisher Link]

[13] P.N. Praveen, and D. Menaka, "A Dual-Axis Solar Tracking System with Minimized Tracking Error through Optimization Technique," *Multimedia Tools and Applications*, vol. 83, no. 20, pp. 58891-58914, 2023. [CrossRef] [Google Scholar] [Publisher Link]

[14] Sanjeev Kumar, Geeta Tiwari, and Neeraj Tiwari, "Evaluating the Impact of Dual-Axis Solar Tracking on Energy Efficiency in Clear Weather," *International Journal of Sustainable Studies, Technologies, and Assessments*, vol. 1, no. 2, pp. 1-15, 2025. [Google Scholar] [Publisher Link]

[15] Ahmed Abdellatif Hamed Ibrahim, SOLTRACK: Dual-Axis Solar Tracking System Dataset, Kaggle, 2024. [Online]. Available: https://www.kaggle.com/datasets/ahmedibra20/soltrack-dual-axis-solar-tracking-system-dataset

[16] Wen Lu, and P. Ajay, "Solar PV Tracking System using Arithmetic Optimization with Dual Axis and Sensor," *Measurement: Sensors*, vol. 33, pp. 1-9, 2024. [CrossRef] [Google Scholar] [Publisher Link]

[17] Alok Sanyal, J.C. Mohanta, and MD Faiyaz Ahmed, "Development of a Dual-Axis Solar Tracker for Efficient Sun Energy Harvesting," *Proceedings of the Institution of Mechanical Engineers, Part E: Journal of Process Mechanical Engineering*, 2024. [CrossRef] [Google Scholar] [Publisher Link]

[18] Sergio I. Palomino-Resendiz et al., "Optimal Selection of the Control Strategy for Dual-Axis Solar Tracking Systems," *IEEE Access*, vol. 11, pp. 56561-56573, 2023. [CrossRef] [Google Scholar] [Publisher Link]

[19] Machrus Ali et al., "The Comparison of Dual Axis Photovoltaic Tracking System using Artificial Intelligence Techniques," *IAES International Journal of Artificial Intelligence*, vol. 10, no. 4, pp. 901-909, 2021. [CrossRef] [Google Scholar] [Publisher Link]

[20] Tabassum Kanwal et al., "An Intelligent Dual-Axis Solar Tracking System for Remote Weather Monitoring in the Agricultural Field," *Agriculture*, vol. 13, no. 8, pp. 1-19, 2023. [CrossRef] [Google Scholar] [Publisher Link]

[21] Hussein A. Kazem et al., "Dual Axis Solar Photovoltaic Trackers: An In-Depth Review," *Energy Sources, Part A: Recovery, Utilization, and Environmental Effects*, vol. 46, no. 1, pp. 15331-15356, 2024. [CrossRef] [Google Scholar] [Publisher Link]

[22] Tuğçe Demirdelen et al., "Performance and Economic Analysis of Designed Different Solar Tracking Systems for Mediterranean Climate," *Energies*, vol. 16, no. 10, pp. 1-23, 2023. [CrossRef] [Google Scholar] [Publisher Link]

[23] Ciptian Weried Priananda et al., "Prototype of Dual Axis Tracking System for Optimization of Energy Harvesting on the Miniature Photovoltaic Array," *2021 International Conference on Advanced Mechatronics, Intelligent Manufacture and Industrial Automation (ICAMIMIA)*, Surabaya, Indonesia, pp. 283-286, 2021. [CrossRef] [Google Scholar] [Publisher Link]

[24] R.Mohamad Idris, Mohammed Ataalah, and Ahmed Abed Mohammed, "Innovative Approaches to Dual Axis Solar Tracking Systems," *Journal of Energy and Safety Technology (JEST)*, vol. 7, no. 2, pp. 112-118, 2024. [CrossRef] [Google Scholar] [Publisher Link]

[25] G.B. Arjun Kumar et al., "Intelligent Two-Axis Solar Tracker for Hybrid Renewable Energy Tree System," *Franklin Open*, vol. 12, pp. 1-10, 2025. [CrossRef] [Google Scholar] [Publisher Link]

[26] Yuvraj Singh et al., "Optimizing Solar Energy Harvesting: Dual-Axis Solar Tracking and Simulation Analysis," *2023 IEEE 3rd International Conference on Applied Electromagnetics, Signal Processing, and Communication (AESPC)*, Bhubaneswar, India, pp. 1-6, 2023. [CrossRef] [Google Scholar] [Publisher Link]

[27] Hayder Abdulsahib Issa et al., "Design, Modeling, and Control of a Dual-Axis Solar Tracker using Fractional Order PID Controllers for Enhanced Energy Efficiency," *Results in Engineering*, vol. 27, pp. 1-14, 2025. [CrossRef] [Google Scholar] [Publisher Link]

[28] Cătălin Alexandru, "Simulation and Optimization of a Dual-Axis Solar Tracking Mechanism," *Mathematics*, vol. 12, no. 7, pp. 1-32, 2024. [CrossRef] [Google Scholar] [Publisher Link]

[29] Diego A. Flores-Hernández et al., "Optimal Strategy for the Improvement of the Overall Performance of Dual-Axis Solar Tracking Systems," *Energies*, vol. 14, no. 22, pp. 1-24, 2021. [CrossRef] [Google Scholar] [Publisher Link]

[30] Cesar Ulises Solís-Cervantes et al., "Design and Implementation of Extremum-Seeking Control based on MPPT for Dual-Axis Solar Tracker," *Mathematics*, vol. 12, no. 12, pp. 1-22, 2024. [CrossRef] [Google Scholar] [Publisher Link]

[31] Ajay Oli et al., "Comparative Study on Efficiency Analysis of Fixed and Dual-Axis Solar Tracking System," *Journal of Engineering and Sciences*, vol. 3, no. 1, pp. 81-86, 2024. [CrossRef] [Google Scholar] [Publisher Link]

[32] Ahmad Al-Othman et al., "An Experimental Study on Hybrid Control of a Solar Tracking System to Maximize Energy Harvesting in Jordan," *Solar Energy*, vol. 263, 2023. [CrossRef] [Google Scholar] [Publisher Link]

[33] Muhammad Fakhry Mohamed Ridzuan et al., "Efficiency Assessments of a Dual-Axis Solar Tracker for Energy Harvesting in Malaysia," *Journal of Advanced Research in Experimental Fluid Mechanics and Heat Transfer*, vol. 19, no. 1, pp. 56-67, 2025. [CrossRef] [Google Scholar] [Publisher Link]